Bacterial defiance as a form of prodrug failure

Authors: Brandon Alexander Holt[1], Isabel Curro[1], and Gabriel A. Kwong[1–5,*]

Affiliations:

[1] Wallace H. Coulter Department of Biomedical Engineering, Georgia Tech College of - Engineering and Emory School of Medicine, Atlanta, GA 30332, USA; [2] Parker H. Petit Institute of Bioengineering and Bioscience, Atlanta, GA 30332, USA; [3] Institute for Electronics and Nanotechnology, Georgia Tech, Atlanta, GA 30332; [4] Integrated Cancer Research Center, Georgia Tech, Atlanta, GA, 30332; [5] Georgia ImmunoEngineering Consortium, Georgia Tech and Emory University, Atlanta, GA 30332.

[*]To whom correspondence should be addressed.

Address: 345 Ferst Dr, Atlanta, GA 30332

Phone: 404-385-3746

Email: gkwong@gatech.edu.

ABSTRACT

Classifying the mechanisms of antibiotic failure has led to the development of new treatment strategies for killing bacteria. Among the currently described mechanisms – which include resistance, persistence and tolerance – we propose defiance as a form of antibiotic failure specific to prodrugs. As a prototypic bacteria-activated prodrug, we construct cationic antimicrobial peptides (AMP), which are charge neutralized until activated by a bacterial protease. Despite prodrug treatment eliminating the vast majority of bacteria populations, we observe defiant phenotypes that survive exposure to identical drug concentrations and durations. Using a multi-rate kinetic feedback model, we show that bacteria spontaneously switch from susceptibility to defiance under disease-related physiological conditions (e.g., hyperthermia, downregulated protease expression). From this model, we derive a dimensionless quantity (Bacterial Advantage Heuristic, *BAH*) – representing the competing rates between bacterial proliferation and prodrug activation – that perfectly classifies bacteria as defiant or susceptible across a broad range of conditions. By recognizing that the switch from susceptibility to bacterial defiance under prodrug treatment behaves analogously to electronic transistors, we construct biological logic gates (e.g., AND, OR, NOT, etc.) to allow assembly of an integrated 3-bit autonomous circuit that universally kills defiant bacteria under all possible combinations of *BAH* values. Here, we study a form of bacterial resistance specific to prodrugs, which reveals universal treatments strategies that can be implemented with biological circuits.

INTRODUCTION

The rise of multidrug-resistant bacteria coupled with the lack of newly developed antibiotics has created a serious public health threat [1, 2]. Understanding the causes of antibiotic failure improves the development of new drugs and informs clinical treatment strategies [3-5]. These failure mechanisms are broadly classified into three distinct categories (i.e., resistance, persistence, and tolerance), which are characterized by the change in drug concentration and exposure time required to kill the bacteria [6]. For example, resistance is characterized by genetic mutations which result in bacteria requiring significantly higher concentrations of antibiotic (minimum inhibitory concentration, MIC) to be lethal. By contrast, bacteria exhibiting tolerance or persistence require increased drug exposure time (minimum duration for killing, MDK), with the latter exhibiting a biphasic killing profile. Further, bacteria populations become tolerant through environmental conditions or genetic mutations, whereas persistence is an actively maintained, non-heritable state exhibited by a subpopulation of bacteria. Discriminating between these survival strategies employed by bacteria is crucial for the development of new drugs and clinical treatment decisions [6].

Antibiotic success is markedly improved by proper drug titration, as overdosing leads to off-target toxicity and underdosing increases the likelihood of pathogens developing resistance[7, 8]. However, ideal drug doses are difficult to achieve over the course of treatment because infection burden changes dynamically over time, creating a moving target[7-9]. Prodrugs, which represent 10% of all FDA-approved drugs in the last decade, are a promising solution because they are automatically titrated by a disease-related activation mechanism and reduce the risk of off-target effects [10]. Prodrugs, such as ganciclovir [11] and sultamicillin [12], are administered as a biologically inactive form and are enzymatically or chemically activated by the diseased cells or pathogens. Here, we create self-titrating prodrugs using cationic antimicrobial peptides (AMP), which evolved as a part of innate immunity and display broad-spectrum and prokaryote-specific antimicrobial

properties [13]. Cationic AMPs act by disrupting bacterial membranes and inducing inflammatory responses [14], but suffer from off-target effects (i.e., toxicity) and low stability *in vivo* [15, 16]. Our AMP prodrugs are activated directly by proteases, a multifunctional class of enzymes that are responsible for regulating important health processes, such as immunity and blood homeostasis, and are major drivers of disease, including cancer and sepsis [17-22]. We chose to target bacterial proteases directly, which are a major cause of virulence [23, 24] during infections and important targets for developing antibiotics [25]. Of these proteases, outer membrane protease T (OmpT), is a membrane-bound bacterial protein that is widely conserved across gram-negative bacteria of the *Enterobacteriaceae* family and recognizes a variety of targets that contribute to virulence (e.g., plasminogen)[26-28]. In this work, we design cationic AMPs that are locked by charge complexation with anionic peptides and connected with a protease-cleavable linker substrate [29, 30]. We create a peptide linker recognized by *E. coli* protease OmpT, such that increasing concentrations of bacteria yield higher concentrations of free drug (**Fig. 1A**).

While this formulation eliminates the majority of bacteria, we observe bacteria populations that we named defiant, which proliferate in the presence of active drug by consistently outpacing prodrug activation at all stages of growth (i.e., log phase, stationary phase). To understand the mechanism by which bacteria become resistant to prodrugs, we built a system of coupled ODEs that model the dynamics of the bacteria-prodrug competition. We use this model to derive the dimensionless quantity – the Bacterial Advantage Heuristic (*B.A.H.*) – which predicts whether bacteria will become defiant under a broad range of conditions. At low *BAH* values, bacteria are susceptible to elimination, but after a critical threshold the bacteria switch to a state of defiance, in which the bacteria proliferate in the presence of activated drug (**Fig. 1B**). To combat this, we design biological circuits that universally treat all conditions (*BAH* values) by recognizing that prodrugs behave analogously to transistors: above a critical *BAH* threshold (i.e., gate voltage), bacteria (i.e., input current) pass through the prodrug and exhibit defiance. Under this definition

of a bit, defiant bacteria represent the 1-state and dead bacteria represent the 0-state. We use this framework to build digital logic gates with prodrug transistors, which operate on multiple *BAH* values and output a binary bacteria population (i.e., living or dead). We arrange multiple AND and NOT gates to construct a circuit that outputs 0 (i.e., dead bacteria) under all eight possible combinations of three input *BAH* values (**Fig. 1D**). These quantitative mechanistic insights will better inform future drug design and treatment protocols leading to antibiotic success.

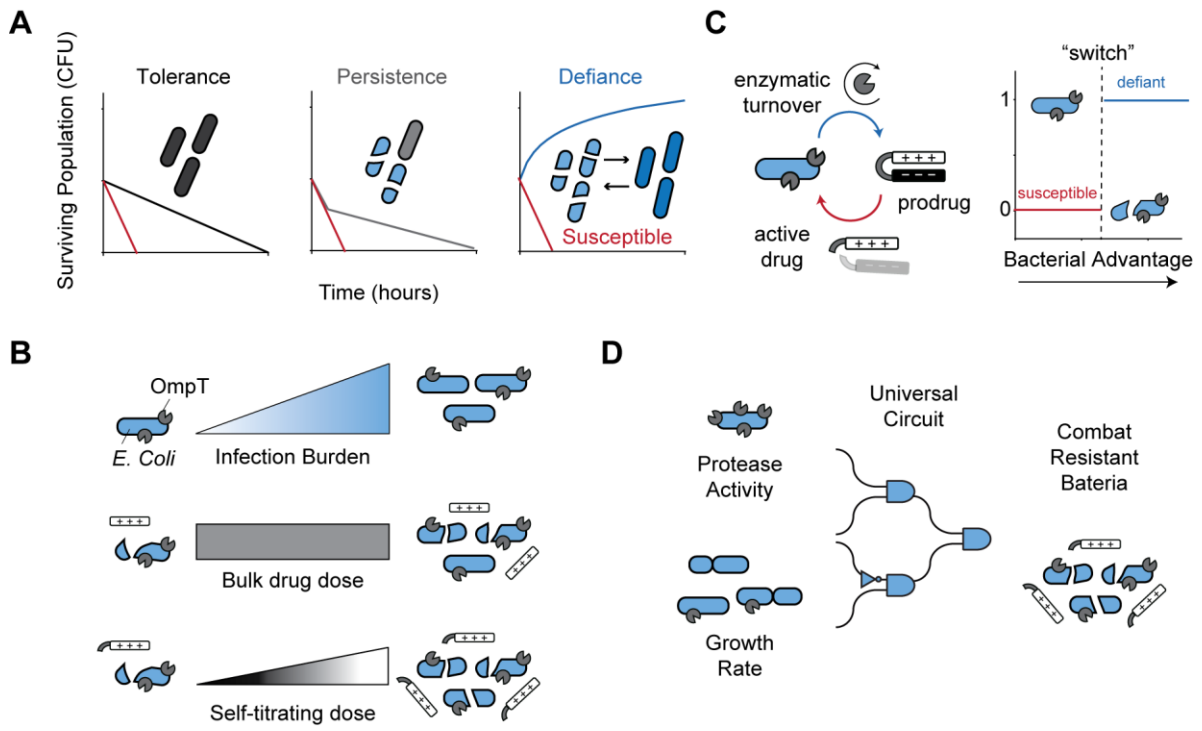

Fig. 1. Bacterial defiance as a form of resistance to self-titrating prodrugs (**A**) Schematic comparing time-dependent killing profiles of bacteria exhibiting tolerance, persistence, or defiance. Red line represents killing profile of susceptible bacteria. (**B**) As infection burden increases (top), a static dose will result in an improper dose (middle). Conversely, a self-titrating drug will unlock an appropriate dose at all infection burdens (bottom). (**C**) Proliferating bacteria either be defiant or susceptible to the prodrug, where the two outcomes are strictly separated by a critical Bacterial Advantage Heuristic (*BAH*) value, resulting in switch-like behavior. (**D**)

Schematic depicting the treatment of resistant bacteria with a universal circuit capable of responding to multiple physiological conditions.

RESULTS & DISCUSSION

Creating a bacterial protease-activated prodrug

To create a bacteria-activated prodrug, we developed an antimicrobial peptide (AMP) that is activated by protease activity. This formulation consisted of a cationic AMP (polyarginine) in charge complexation with anionic peptide locks (polyglutamic acid) to create an inactive form of the AMP[29]. The drug (polyarginine) and lock (polyglutamic acid) were connected with a linker peptide (RRSRRV) that is unlocked by a bacterial protease (OmpT) upon proteolytic cleavage, creating a precise mechanism for self-titration (**Fig. 2A**). To demonstrate the specificity of OmpT for the chosen linker peptide sequence, we synthesized a fluorogenic peptide containing a fluorescence-quencher pair[27] and detected OmpT activity in samples incubated with recombinant OmpT or live *E. coli* culture. Further, we demonstrated the ability to turn off OmpT activity with the serine protease inhibitor, Aprotinin, which exhibits inhibitory effects in the micromolar range[26] (**Fig. 2B**). Using this substrate, we confirmed that the proteolytic cleavage of this substrate linker also occurred when docked on the drug-lock complex, which presents a different conformational state of the peptide substrate (**Fig. 2C**). To determine the MIC of the unlocked drug, we showed that bacteria dosed with free drug show no growth in comparison to bacteria alone (**Fig. 2D, E**). Dosing locked prodrug at this concentration, we used an orthogonal protease (Tobacco Etch Virus Protease) substrate pair to show the drug is only activated to kill bacteria in the presence of the correct target protease. We then used the prodrug locked with the OmpT substrate to show that the drug is only activated in the presence of bacterial protease activity. In the presence of the prodrug, all bacteria were eliminated whereas in the presence of the prodrug and the OmpT

inhibitor, Aprotinin, bacteria proliferated at the same rate as the bacteria alone control (**Fig. 2D, E, Table S1**). To summarize, we designed charge neutralized cationic peptides that behave as prodrugs when activated by the bacterial protease, OmpT.

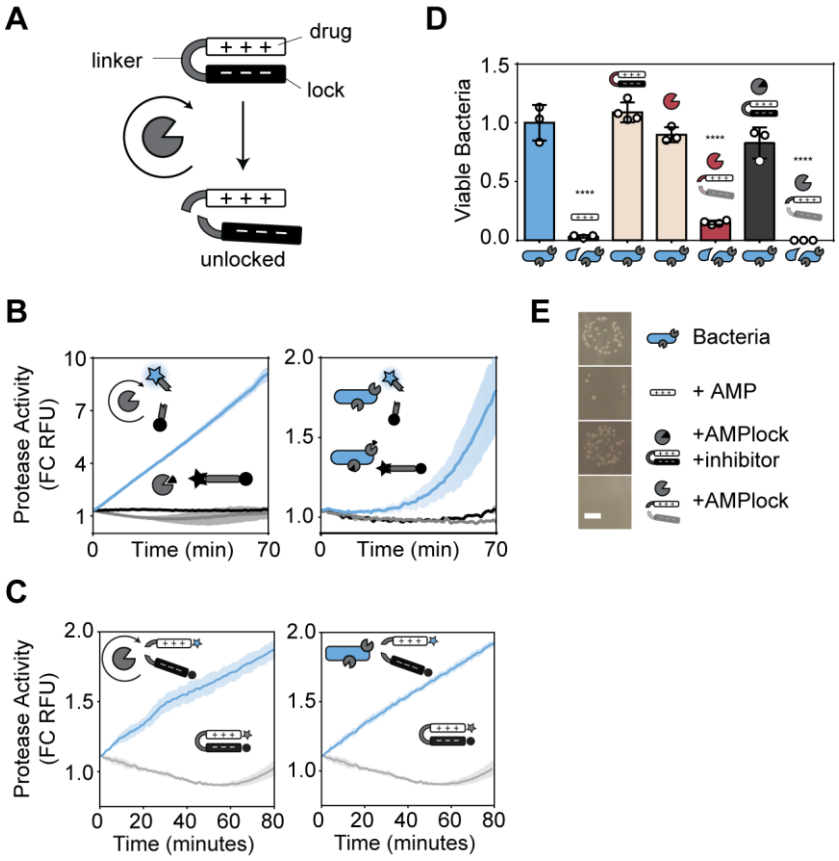

Fig. 2. A bacteria-activatable prodrug targets *E. coli* protease OmpT (**A**) A cationic AMP (drug) locked by an anionic peptide (lock) with a protease-cleavable linker is activated by enzyme activity. (**B**) Cleavage assay measuring recombinant OmpT (grey protease) activity (left) and OmpT expressed by live E. coli (right) against a fluorescent quenched peptide substrate (blue lines). (**C**) Cleavage assay measuring recombinant OmpT (left) and OmpT expressed by E. coli (right) against fluorescently labeled locked prodrug. Negative control is with the addition of inhibitor aprotinin (black triangle, black lines). Probe only control (grey lines). Shading represents standard deviation (n = 3). All cleavage assays plotted as fold change in RFU from initial time point. (**D**) Bacteria viability assay quantifying the cytotoxic effect of the AMP-locked drug in the

presence of the cognate active protease (TEV protease is red; OmpT is grey). All values normalized to bacteria only control and plotted as fraction. Error bars represent standard deviation (n = 3). (**E**) Figure legend and representative images of bacterial plates used for estimating viability (scale bar = 4 mm). * < 0.05, ** < 0.01, *** < 0.001, and **** < 0.0001.

Bacteria-prodrug kinetic model

The bacteria-activated prodrug leveraged protease activity to enable auto titration according to a rate constant (i.e., activated drug concentration per time), which is a function of system parameters such as enzymatic efficiency (k_{cat}/K_m) and bacterial growth rate (*r*). To quantitatively understand how the rate of prodrug activation competes with the number of living bacteria, we built a mathematical model using a system of nonlinear ordinary differential equations (ODE). In this model, the prodrugs create a negative feedback loop, where bacteria activate prodrugs, which in turn inhibit bacterial growth (**Fig. 3A**). We modeled the growth of the bacteria population, *B*, with a standard logistic growth model [31], where B_{max} determines the bacterial carrying capacity (maximum concentration of bacteria) and the growth rate, *r*, determines the speed at which the population approaches B_{max}. The decay of the bacteria population is a function of the concentration of unlocked drug, *U*, and the amount of drug needed to kill bacteria per unit time, *a* (**Table S2, Equation 1.1**).

$$\frac{dB}{dt} = rB\left(1 - \frac{B}{B_{\max}}\right) - \frac{U}{a} \tag{1.1}$$

The drug is unlocked by enzymatic activity, so we modeled the decay of the available locked drug, *L,* with standard Michaelis-Menten kinetics where the catalytic rate of the reaction and the half-maximal substrate concentration are determined by k_{cat} and K_m, respectively (**Equation 1.2**). We

defined one bacterium, with ~ 2.5×10^3 OmpT proteases per cell [32], as equivalent to one effective enzyme to reflect the valency of protease active sites on each bacterial membrane.

$$\frac{dL}{dt} = -k_{cat} B \frac{L}{K_m + L} \tag{1.2}$$

The conversion from locked to unlocked drug, *U,* is conserved, so the decay of locked drug directly translates to the growth of unlocked drug. The unlocked drug decays, a^*, due to aggregation with dead bacteria membranes, for which we used published values [33] (**Equation 1.3**).

$$\frac{dU}{dt} = k_{cat} B \frac{L}{K_m + L} - \frac{a^*}{a} U \tag{1.3}$$

To fit this model to our data, we measured the parameters included in the model, including drug cytotoxicity (e.g., *EC50, a*), enzymatic efficiency (e.g., k_{cat}, K_m), and bacterial growth rate (*r*) (**Fig. S1A-C**). Using these values (**Table S2**), the model showed that after a period of initial bacterial growth, the lagging drug population ultimately eliminated the bacteria. While the initial reservoir of locked drug concentration was ~200 µM, the unlocked drug never rose above 5 µM (**Fig. S1D**), revealing that this system maintains the minimal drug concentration required to kill the infection. To apply this model to a broad range of prodrugs, we developed a general form of the prodrug-disease target model based on well-established pharmacokinetic parameters (**Fig. S2**).

Predicting bacterial defiance with a dimensionless constant

While it is advantageous for prodrugs to minimize the concentration of active drug, we show that this enables defiant populations of bacteria to appear under certain circumstances. We hypothesized that a critical relationship between the system parameters (e.g., k_{cat}/K_m, *r,* etc.) determines whether bacteria become defiant. Using Buckingham Pi theorem, we derived a

dimensionless quantity representing the balance between growth rate (*r*) and enzymatic turnover (k_{cat}/K_m), which we define as the Bacterial Advantage Heuristic (*B.A.H.*) (**Equation 1.4**).

$$B.A.H. = \log_{10}\left(\frac{r / B_{\max}}{k_{cat} / K_M}\right) \tag{1.4}$$

Under this definition, bacteria became defiant when they reach a critical *BAH* value, through physiological or environmental changes. For example, as the bacteria grew faster (*r*), *BAH* increased because the bacteria were more likely to multiply before being killed by an activated drug. Conversely, the *BAH* decreased as bacterial enzyme activity (k_{cat}/K_m) increased, because the bacteria were more likely to unlock a larger quantity of drug before dying.

To find the critical *BAH* threshold that determined defiance, we set up nine different environmental conditions, each with a unique combination of k_{cat}/K_m and *r* values, which we controlled with ambient temperature, broth concentration and protease inhibitors. We incubated bacteria with the previously developed fluorophore-quencher probe (**Fig. 2B**) to monitor bacterial protease activity over time in each of the nine conditions. To quantify *r*, k_{cat}/K_m and *BAH*, we fit a simplified model of logistic bacteria growth and enzymatic turnover in a system with no prodrug (**Fig. S3A, Table S2**, **Equations S1.7, S1.8**). To measure the outcome of bacteria populations exposed to the prodrug, we set up the same nine environmental conditions with the addition of the prodrug. We found experimentally that the final bacteria population (i.e., steady-state value) was binary: either 0 or B_{max} (**Fig. 3B**). Therefore, a population of bacteria in the presence of a prodrug will converge to either susceptibility (death) or defiance (survival), which was also confirmed analytically (**Fig. 3C, Equations S1.9, 1.10**). To validate our model, we made serial CFU measurements, which closely matched the bacterial growth predicted by our simulations in each of the nine conditions (**Fig. 3D, Fig. S3B, Table S3**). To computationally predict the critical *BAH* threshold, we simulated 10^4 unique *BAH*s by varying *r* and k_{cat}/K_m across four orders of magnitude and comparing to the simulated outcome (BAH_{crit} = 3.261). We confirmed this result

experimentally by plotting live/dead results versus *BAH* from each of the nine conditions, which revealed a sharp step function near the same critical value (BAH_{crit} = 3.17—3.44) (**Fig. 3E**). When using the *BAH* as a binary classifier of this system, we perfectly predicted the onset of bacterial defiance under a set of 13 unique environmental conditions (**Fig. 3F, G**). Further, we demonstrated the ability to switch defiant bacteria to a state of susceptibility by changing the amino acid sequence of the peptide linker, increasing k_{cat}/K_m (**Fig. S4**). Taken together, these results show that insights gained from a non-dimensional value can improve prodrug success using design principles guided by a dimensionless quantity, *BAH*.

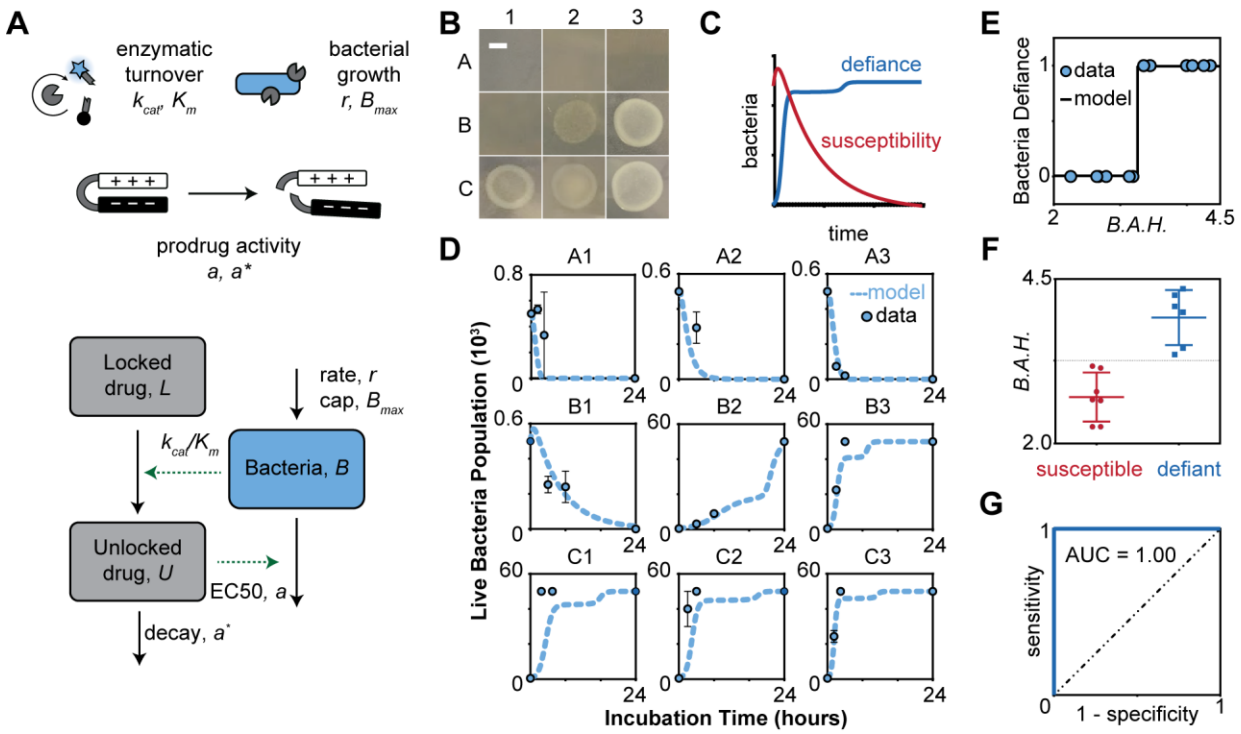

Fig. 3. Predicting bacterial defiance with a dimensionless constant (**A**) Graphical representation of the model of bacteria and unlocked drug populations. Legend describes the agents associated with each variable. (**B**) Agar plates showing presence/absence of bacterial growth and end-point for nine environmental conditions (A1—C3, scale bar = 4 mm). (**C**) Schematic depicting that bacterial defiance is characterized by proliferation in the presence of activated drug. (**D**) Validating the model with serial CFU measurements (error bars SEM) and

ODE model simulations of nine conditions given extracted growth rate and enzyme kinetics parameter values. (**E**) Correlating BAH with bacteria outcome to measure critical defiance value. (**F**) Grouping bacteria populations into defiant and susceptible based on *BAH*. (**G**) Using *BAH* to classify populations as defiant based on bacteria-driven parameters (r and k_{cat}/K_m).

Building logic gates with prodrug transistors

We sought to leverage the binary properties of these prodrugs to design a biocircuit capable of universally treating bacterial defiance. We accomplished this by recognizing that certain prodrugs behave analogously to electronic transistors. Transistors allow input current (I_{in}) to pass (I_{out}) when the gate voltage (G) is above a defined threshold; similarly, prodrugs allow input bacteria (B_{in}) to survive (B_{out}) when the *BAH* is above a critical value (**Fig. 4A**). Within computers, transistors are arranged in small circuits to create digital logic gates, which are in turn combined to form larger circuits that perform sophisticated tasks. We sought to emulate this hierarchical structure and leverage the transistor-like behavior of prodrugs to create a circuit capable of combatting bacterial defiance, which required transistors as well as NOT gates. In contrast to a transistor, a NOT gate kills bacteria when *BAH* = 1, and allows bacteria to survive when *BAH* = 0 (**Fig. 4B**). To create a NOT gate, we used heat triggered liposomes[34] that release drugs when heated above 37C (**Fig. S5**). When exposed to temperatures above 37C, which correspond to *BAH* = 1, the liposomes released the drugs, killing bacteria, whereas lower temperatures (i.e., *BAH* = 0) allowed bacteria to survive (**Fig. 4B**). These results demonstrate the function of prodrugs as bacterial transistors or NOT gates, which can be arranged in simple circuits to create digital logic gates.

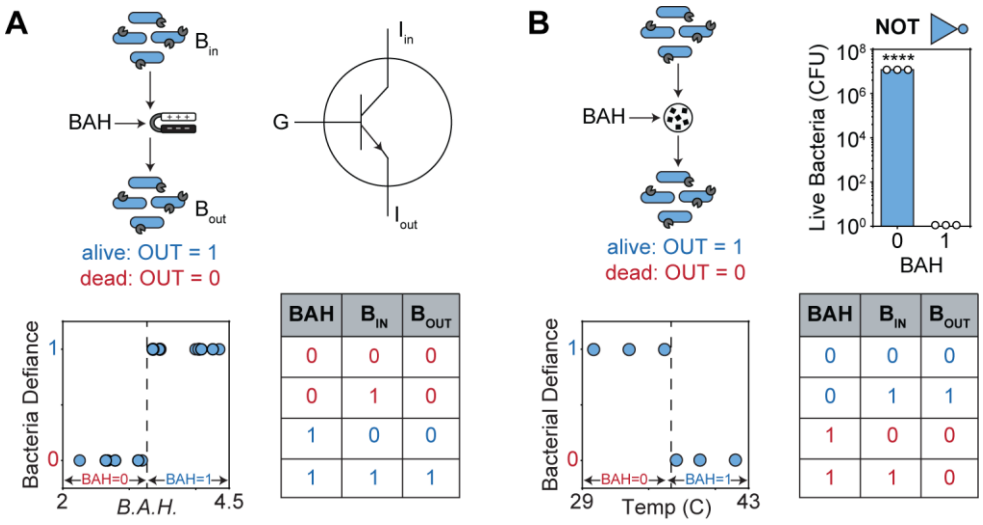

BAH	B_{IN}	B_{OUT}
0	0	0
0	1	0
1	0	0
1	1	1

BAH	B_{IN}	B_{OUT}
0	0	0
0	1	1
1	0	0
1	1	0

Fig. 4. Building logic gates with prodrug transistors (**A**) Schematic and truth table showing how prodrugs behave analogously to transistors, in which the passing of an input signal (I_{in}, B_{in}) is determined by a gate signal (G, BAH). (**B**) Schematic depicts heat-triggered, drug loaded (black squares) liposomes (black circle). Bacterial viability assay (bar graph) validating the function of a prodrug-based NOT gate. Fluorescent assay (scatter plot) measuring the release of FITC from heat-triggered liposomes. Data binarized based on threshold, where release of cargo is defiance (1) and no release of cargo will not kill bacteria (0). All truth tables depict ideal binary input-output combinations. Error bars represent standard deviation (n = 3) * < 0.05, ** < 0.01, *** < 0.001, and **** < 0.0001.

Combatting bacterial defiance with an autonomous, universal circuit

The goal of programmable medicine is to design autonomous biological circuits capable of diagnosing and treating disease. We sought to leverage the transistor-like behavior of prodrugs to combat the problem of bacterial defiance. We proposed a set of three environmental inputs described by *BAH* values (i.e., BAH_A, BAH_B, and BAH_C), which were each controlled with different system parameters (i.e., media concentration, temperature, and substrate sequence). We

computationally generated 32 candidate circuits that produce the output 0 under all eight combinations of input conditions and only use AND, OR, or NOT gates. We chose a simple circuit, which uses 3 AND gates and 1 NOT gate (**Fig. 5A, B**). To create AND gates with prodrugs, we mirrored the arrangement of electronic transistors by placing two prodrugs, each with an associated *BAH* input (i.e., BAH_A *and* BAH_B) in series by sequentially dosing the bacteria (**Fig. 5C**). For this example, we used two drugs with different substrate specificities, where the substrate with high k_{cat}/K_m corresponds to *BAH* = 0 and the substrate with low k_{cat}/K_m corresponds to *BAH* = 1. When exposed to all four possible inputs (i.e., 00, 01, 10, and 11), bacteria only survived the 11 condition, creating an AND gate function (**Fig. 5C**). Whereas the AND gate was created with prodrugs in series, we recapitulated the OR gate by arranging two prodrugs in parallel. Using this circuit, bacteria survived in any case where at least one input *BAH* = 1, creating an OR gate function (**Fig. 5D**). To create the universal circuit (**Fig. 3A**), we mixed a cocktail of 3 AND gates and 1 NOT gate and applied this circuit to all eight possible input conditions. Whereas a single prodrug only eliminated bacteria in about half of the input cases (**Fig. 5E**), our circuit autonomously eliminated bacteria in all possible combinations (**Fig. 5F**). Here, we augment prodrugs with the capacity to respond to a broad range of physiological conditions. In addition to self-dosing, programmable prodrugs have the potential to universally respond to different biological states.

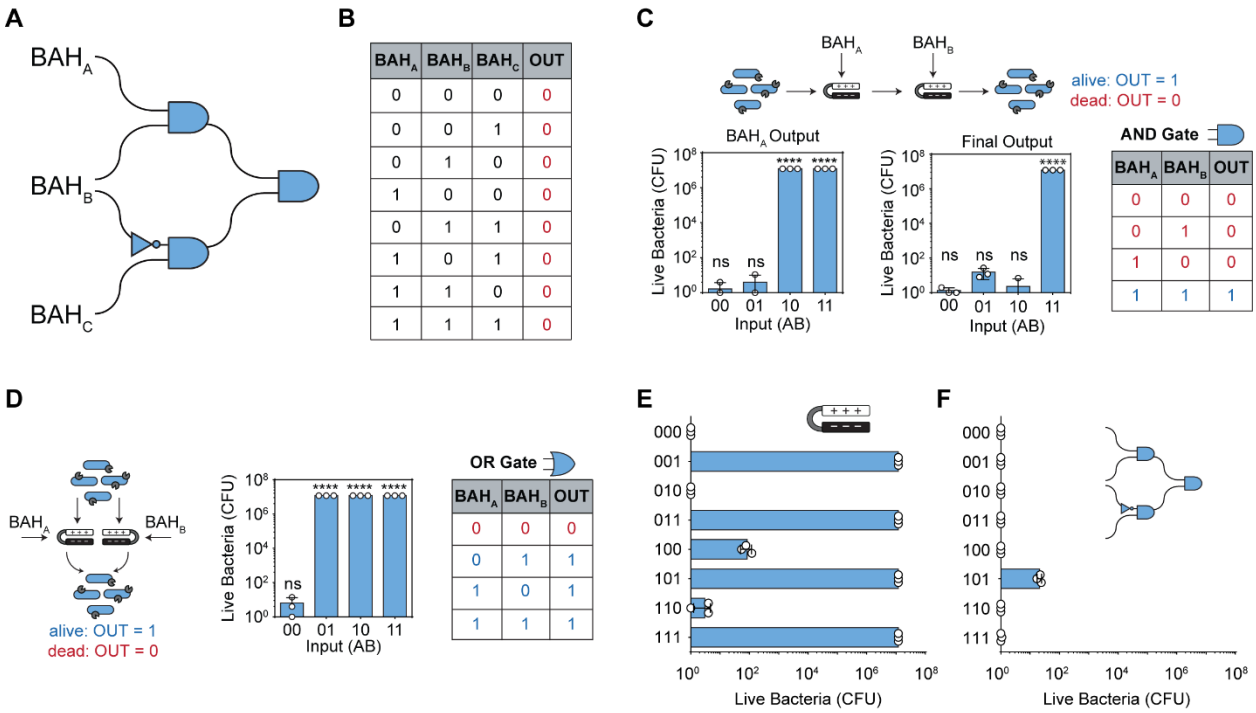

Fig. 5. Combatting bacterial defiance with an autonomous, universal circuit. (**A**) Logic circuit schematic depicting a function that universally outputs 0 for all possible combinations of three binary inputs. (**B**) Truth table for universal circuit input-output combinations. (**C**) Bacterial viability assay validating the function of a prodrug-based AND gate. Schematic depicts two prodrug transistors arranged in series. (**D**) Bacterial viability assay validating the function of a prodrug-based OR gate. Schematic depicts two prodrug transistors arranged in parallel. (**E**) Bacterial viability assay quantifying the outcome of a single prodrug in the context of different environmental conditions. (**F**) Bacterial viability assay demonstrating the eight outputs of the autonomous circuit. All truth tables depict ideal binary input-output combinations. Error bars represent standard deviation (n = 3). * < 0.05, ** < 0.01, *** < 0.001, and **** < 0.0001.

CONCLUSION

While these findings complement existing knowledge about bacterial mechanisms that cause antibiotic failure, prodrugs introduce a unique element: the competition between bacterial growth and prodrug activation. To understand this behavior, we establish bacterial defiance as a form of antibiotic failure which allows bacteria to proliferate while activating prodrugs. To study bacterial defiance, we created an OmpT-activatable AMP prodrug with the ability to localize its activity to *E. coli* membranes and elicit precise titration. This formulation can be applied to other diseases by designing a peptide linker specific to a disease-related protease. We established a mathematical framework for determining the mechanism of defiance for bacteria and general diseases. Under this framework, measurable system parameters determine whether bacteria will become defiant in the presence of a particular prodrug. Our model reveals that there are many parameters, including drug half-life and temperature, that can be controlled to improve prodrug efficacy. In addition to the environmental conditions studied in this work, there are established genetic mutations in *E. coli* capable of causing defiance. For example, mutations resulting in partial reduction or total loss of OmpT activity [35, 36] as well as changes in growth rate [37] have been identified in *E. coli*.

The proposed framework for characterizing defiance will enable more conscious engineering of prodrugs and provide strategies for combatting antibiotic failure. By creating an autonomous circuit that kills bacteria in a variety of physiological conditions, we demonstrate an ideal template for administering prodrugs in the context of defiant populations of bacteria. Prodrugs are already a promising strategy for combatting antibiotic failure, because they are self-dosing and reduce off-target effects[10]. By engineering prodrugs treatments with logically controlled circuits, future treatments will also be able to universally respond to different physiological states. Under the paradigm of programmable medicine, augmented prodrugs may prove to combat the growing problem of antibiotic resistance.

Author Contributions: G.A.K. and B.A.H conceived of the idea. G.A.K, B.A.H., and I.C. designed experiments and interpreted results, and wrote the manuscript. B.A.H. and I.C. carried out experiments.

Acknowledgments: This work was funded by an NIH Director's New Innovator Award (Award No. DP2HD091793). B.A.H is supported by the NSF GRFP, National Institutes of Health GT BioMAT Training Grant under Award Number 5T32EB006343 and the Georgia Tech President's Fellowship. This material is based upon work supported by the National Science Foundation Graduate Research Fellowship under Grant No. DGE-1650044 (B.A.H.). G.A.K. holds a Career Award at the Scientific Interface from the Burroughs Welcome Fund. The content is solely the responsibility of the authors and does not necessarily represent the official views of the National Institutes of Health. The authors would like to thank Ian Miller (Georgia Tech), Shreyas Dahotre (Georgia Tech), and Dr. Kyle Allison (Georgia Tech & Emory) for their helpful discussion.

EXPERIMENTAL PROCEDURES

Protease Cleavage Assays

All protease cleavage assays were performed with a BioTek Cytation 5 Imaging Plate Reader, taking fluorescent measurements at 485/528 nm (excitation/emission) for read-outs measuring peptide substrates terminated with FITC (Fluorescein isothiocyanate). Kinetic measurements were taken every minute over the course of 60 – 120 minutes at 37 C. Tobacco Etch Virus protease (TEVp), along with its substrate and buffer was obtained from Anaspec, Inc. (Fremont, CA). Activity RFU measurements were normalized to time 0 measurement, and as such represent fold change in signal. Outer Membrane Protease T (i.e., OmpT, Protease 7) was purchased from Lifespan Biosciences (Seattle, WA). OmpT fluorescent peptide substrate was custom ordered from Genscript (Piscataway, NJ).

Bacterial culture and cytotoxicity measurement

DH5α Escherichia coli were a gift from Todd Sulchek's BioMEMS lab at Georgia Tech. E. coli were cultured in LB broth (Lennox) at 37 C and plated on LB agar (Lennox) plates. LB broth was purchasd from Millipore Sigma (Burlington, MA) and LB agar was purchased from Invitrogen (Carlsbad, CA). AMP and locked AMP were custom ordered from Genscript (Piscataway, NJ). See Table S1 for more information. Bacteria were grown to a concentration of 10^9 CFU/mL before being used for experiments. Concentration was estimated by measuring the OD_{600} of the bacterial suspension, and assuming an OD_{600} of 1.000 corresponds to a concentration of 8×10^8 CFU/mL. Bacterial cell viability was measured by making eight 10-fold serial dilutions, and plating three 10 uL spots on an LB agar plate. Plates were incubated overnight at 37C, and CFUs were counted. Untreated bacteria CFU counts served as control for 0% cytotoxicity, and bacteria + IPA (or 0 countable CFUs) served as control for 100% cytotoxicity.

Liposome Preparation

DPPC and MPPC were purchased from Avanti Polar Lipics, inc. The heat-triggered NOT gate formulation was composed of DPPC:MPPC at the molar ratio 9:1, and were evaporated in cholorform to produce a lipid film. Films were rehydrated in 100% water containing 100 mg/mL ampicillin and were sonicated for 20 minutes. Lipid formulations were then purified using a PD-10 desalting column (GE Healthcare) and size was measured via dynamic light scattering (DLS, Malvern).

Computational model

The ODE modelling and solutions were performed in MATLAB 2016b. Code can be found in supplementary information.

Statistical Analysis

Statistical analysis was performed using statistical packages included in GraphPad Prism 6. To assess the significance of increase in signal due to protease cleavage, we used a two-way ANOVA (without repeated measures) followed by Sidak's multiple comparisons test. A one-way ANOVA followed by Dunnett's multiple comparisons test was used to compare experimental means to cells only control bacterial viability assays. Two-way ANOVA followed by Sidak's multiple comparisons test used to compare experimental means to control for bacterial cytotoxicity at multiple starting concentrations.

SUPPLEMENTARY INFORMATION, FIGURES, AND TABLES

Measuring kinetic parameters for the ODE model

To measure drug cytotoxicity, we quantified the percent of viable bacteria when exposed to unlocked AMP drug doses ranging from nanomolar to millimolar concentrations and observed a spike in cytotoxicity in the micromolar range (**Fig. S1A**). To calculate bacterial growth rate constants, we incubated bacteria in broth or water at 37C and measured OD_{600} over the course of 8 hours, revealing a higher growth rate in broth consistent with published values[31, 37] (3.0 > 0.1 h^{-1}) (**Fig. S1B**). To quantify enzymatic velocity, we measured proteolytic velocity (moles L^{-1} s^{-1}) under substrate concentrations ranging from 0—200 uM and fit the Michaelis-Menten equations to this data to calculate k_{cat} and K_m (**Fig. S1C**). Using these measured parameters (**Table S2**), we generated kinetic curves for bacteria number and drug concentration over time. The model showed that after a period of initial bacterial growth, the lagging drug population eliminated the infection burden. While the initial reservoir of locked drug concentration was ~200 µM, the unlocked drug never rose above 5 µM (**Fig. S1D**), revealing that this system maintains the minimal drug concentration required to kill the infection.

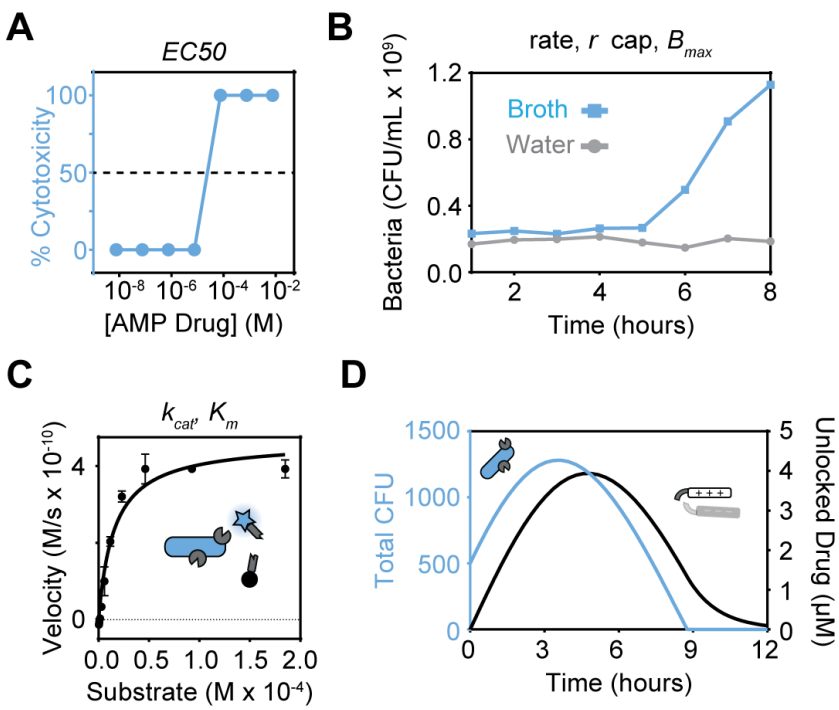

Fig. S1. Creating a bacteria prodrug ODE model. (**A**) EC50 measurement on a sample of *E. coli* exposed to increasing concentrations of AMP. (**B**) Growth rate calculation of *E. Coli* in broth and water by measuring OD at 600 nm. (**C**) Measuring k_{cat}/K_m from a series of cleavage assays incubating *E. coli* at a range of substrate concentrations. (**D**) Predicting the dynamics of the bacteria and unlocked drug population given empirical parameter values. Error bars are standard deviation (n = 3).

A generalized model of disease-triggered prodrugs.

To apply the concept of bacterial defiance to a broad range of prodrugs, we developed a general form of the prodrug-disease target model. This model did not depend on the mechanism of action (**Fig. S2A**) and raised each variable to an arbitrary power to allow for both linear and non-linear processes. In this system, we described a disease (*D*) which converts a prodrug (*P*) into an active form (*A*) by an arbitrary mechanism (**Equations S1.1—S1.3**):

$$\frac{dD}{dt} = a\left(1-\left(\frac{D}{D_{\max}}\right)^{n}\right) - bA \qquad \text{(S1.1)}$$

$$\frac{dP}{dt} = -cD^n P^n \tag{S1.2}$$

$$\frac{dA}{dt} = cD^n P^n - dD^n A^n \tag{S1.3}$$

We defined four generalized parameters: disease expansion rate (*a*), drug efficiency (*b*), drug activation rate (*c*), and drug decay (i.e., metabolism and excretion, *d*), which are well-established pharmacokinetic parameters for prodrugs. We defined a boundary condition based on the constraint that total drug concentration (i.e., prodrug + active drug) is always decreasing and is therefore less than the initial prodrug concentration, which must hold true for any time, *t* (**Equation S1.4**).

$$\begin{gathered} A(t) + P(t) \le P(t=0) \\ A_{ss} + P_{ss} \le P_0 \end{gathered} \tag{S1.4}$$

By substituting the steady state values of *A* and *P* when *D* converges to 0, we defined an inequality that holds true when the disease is susceptible to the prodrug (i.e., $D_{ss} = 0$) (**Equation S1.5**).

$$\left(\frac{a}{b}\right)^{1/n} + \left(\frac{ad}{bc}\right)^{1/n} \le P_0 \tag{S1.5}$$

Therefore, when the collective values of *a, b, c,* and *d* contradict this inequality, the disease will reach carrying capacity (D_{max}), which is a state of defiance. Using this condition, we defined a dimensionless group, the General Advantage Key (*GAK*), which predicts the critical point at which diseases switch to a state of defiance (**Equation S1.6**).

$$B.A.H._{general} = \ln\left[\frac{1}{P_0}\left(\frac{a}{b}\right)^{1/n} + \left(\frac{ad}{bc}\right)^{1/n}\right] > 0 \tag{S1.6}$$

Therefore, high disease growth rates (*a*) and drug decay (*d*), coupled with low drug efficacy (*b*) and disease activity (*c*), result in defiance (*GAK* > 0). Our simulations showed that when the initial

prodrug was considered non-limiting (i.e., $P_0 \gg {}^{ad}/_{bc}$), the disease switched states precisely at *GAK* = 0, but at limiting concentrations of P_0, susceptible diseases moving slowly towards elimination survived because the prodrug resource was depleted. As the starting amount of prodrug decreased, a larger fraction of systems with *GAK* < 0 entered the defiant state creating phase shifted step-functions. As we decreased P_0, the system entered the drug-limited regime faster for larger values of ${}^{ad}/_{bc}$, resulting in larger phase shifts (**Fig. S2B**). We extended the generalizability of this model to prodrug systems that operate under nonlinear processes and confirmed computationally that higher order models produce the same switch-like behavior centered around *GAK* = 0 (**Fig. S2C**). These parameters are fundamental pharmacokinetic quantities, which are measured for any FDA-approved prodrug. We envision the *GAK* to be used a guiding principle for designing prodrugs that combat antibiotic failure.

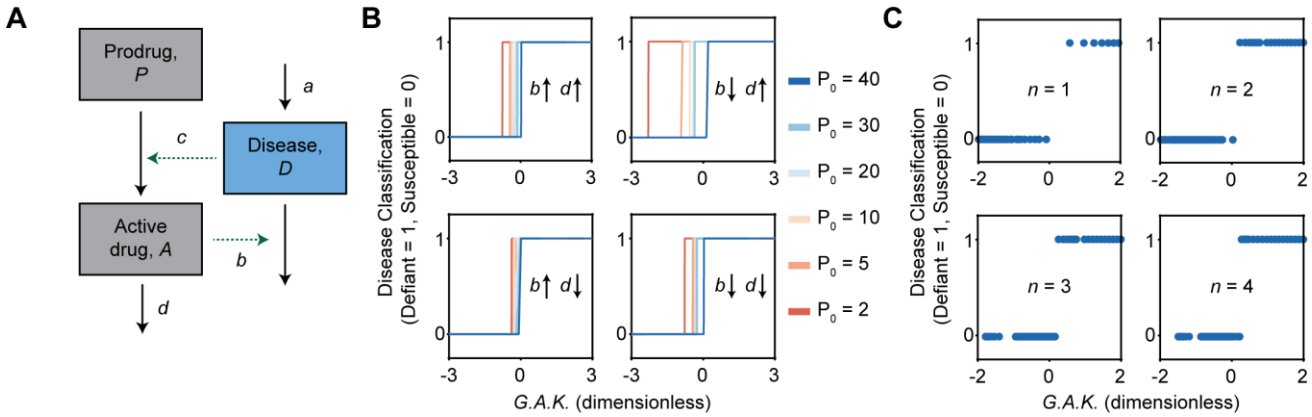

Fig. S2. A generalized model of disease-triggered prodrugs. (**A**) Schematic of generalized model of disease activated prodrug, with parameters *a* (disease growth), *b* (drug EC50), *c* (drug kinetics), and *d* (drug decay). (**B**) Computationally predicted disease outcomes from general form model, using *GAK* as a predictor for disease outcome. Each panel indicates the relative value of ${}^{ad}/_{bc}$ by increasing or decreasing *b* and *d* three-fold. Line color shifts from blue to red indicate decreasing amount of starting prodrug (P_0). (**C**) Simulating higher order nonlinear models to identify the value of *BAH* at which the system switches states.

Estimating bacterial growth rate and enzymatic activity with parameter fitting

To estimate bacterial growth rate (r) and enzymatic efficiency (k_{cat}, K_m), we used parameter fitting methods to a simplified model without a prodrug (**Fig. S3A**). In this model, the prodrug is substituted with a fluorescent probe (P), which is activated with the same substrate sequence as the AMP prodrug. The concentration of cleaved fluorescent probe is monitored over time, and the bacterial concentration is quantified at serial time points. We fit this data to the two equations modelling bacterial growth and activation of the fluorescent probe (**Equations S1.7, 1.8**).

$$\frac{dB}{dt} = rB\left(1 - \frac{B}{B_{\max}}\right) \tag{S1.7}$$

$$\frac{dP}{dt} = -k_{cat} B \frac{P}{K_m + P} \tag{S1.8}$$

We found experimentally that the final bacteria population (i.e., steady-state value) was binary: either 0 or B_{max}. This is confirmed analytically because the steady state value of U_{ss} is always 0, so the steady state value of B only has two possible values (**Equation S1.9, 1.10**).

$$0 = B' = rB_{ss}\left(1 - \frac{B_{ss}}{B_{\max}}\right) \tag{S1.9}$$

$$B_{ss} = 0, B_{\max} \tag{S1.10}$$

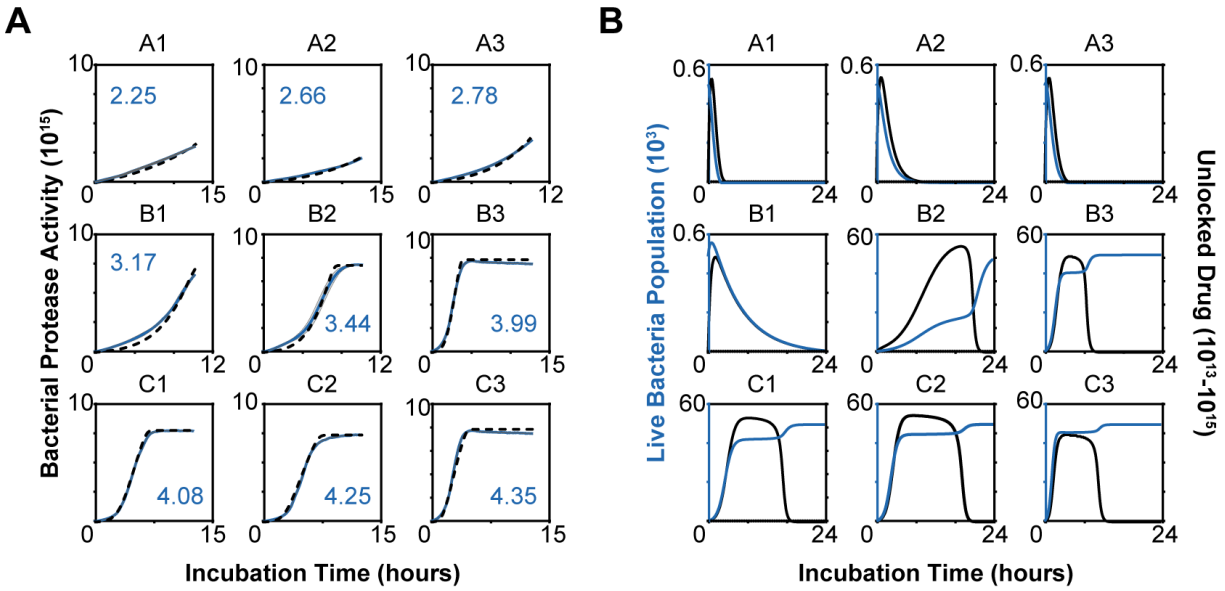

Fig. S3. Modeling bacteria and drug kinetics. (**A**) Bacterial cleavage assays (blue line), from which growth rate (r) and enzyme kinetics (k_{cat}/K_m) are extracted, and *BAH* is calculated (inset). Dotted line represents model after parameter fitting. (**B**) ODE model of bacteria (blue line) and unlocked drug populations (black line) over 24 hours for nine environmental conditions.

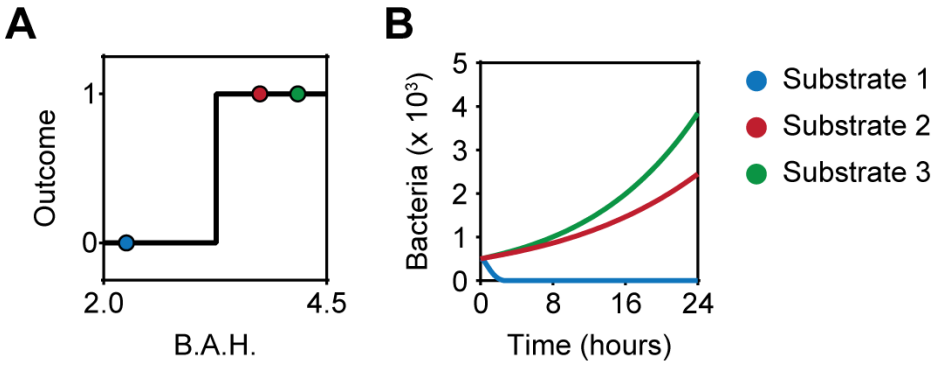

Fig. S4. Altering drug efficacy with substrate affinity. (**A**) Bacteria viability outcome post 24 hour incubation with drug unlocked by substrate two and three. B.A.H. values extrapolated from bacteria + probe velocity measurements fitted to model. (**B**) Bacteria dynamics predicted by model given three different enzyme kinetics.

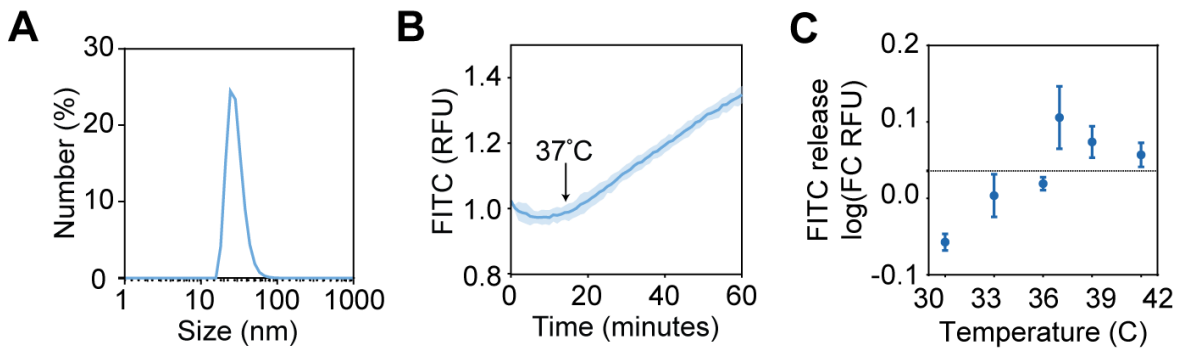

Fig. S5. Validating heat-triggered liposomes. (**A**) Dynamic light scattering of liposome formulation to determine particle size (~35 nm). Histogram is plotted as the mean of independent measurements (n = 3). (**B**) Fluorescent assay measuring the heat-triggered release of liposome contents. Liposomes were loaded with 100 mM FITC, and heated from 25 C to 37C (indicated by arrow). Lines are plotted as means of independent measurements, shading represents standard deviation (n = 3). (**C**) Fluorescent assay measuring the release of FITC from heat triggered liposomes at various temperatures. All samples were heated to 30 C for 10 minutes, then heated at the plotted temperature for 30 minutes. Measurements are plotted as fold change in RFU between final measurement and measurement at 30 C. Error bars represent standard deviation (n = 3).

TABLE S1

Name	Peptide Sequence
Locked AMP (substrate 1)	EEEEEEEEEEEEERRSRRVRRRRRRRRR
Locked AMP (substrate 2)	EEEEEEEEEEERKTRRRRRRRRR
Locked AMP (substrate 3)	EEEEEEEEENLYFQGRRRRRRRRRR
Locked AMP Probe	DABCYL-EEEEEEEEEEEEERRSRRVRRRRRRRRR[Lys(5-FAM)]
OmpT Probe	DABCYL-RRSRRV-Lys(5-FAM)

TABLE S2

Variable	Value	Units	Notes
r	0.1—3	h^{-1}	Bacterial growth rate
kcat	1—25e10	h^{-1}	Enzyme catalytic turnover
Km	4.5e14	[n] in 50 µL	Michaelis constant
Bmax	50,000	[n], bacteria	Bacteria carrying capacity
a	1e11	h^{-1}, AMP/bacteria/hr	Cytotoxic efficiency, EC50
a^*	2.4e11	AMP/bacteria	AMP decay

TABLE S3

Location (row, column)	Temperature	LB Broth Concentration	r (h^{-1})	k_{cat} (h^{-1}) x 10^{10}
1,1 (A1)	37C	0%	0.1	25
1,2 (A2)	30C	2%	0.14	13.6
1,3 (A3)	37C	2%	0.3	22
2,1 (B1)	37C	4%	0.5	15
2,2 (B2)	37C	6%	0.85	13.6
2,3 (B3)	37C	20%	2.2	1
3,1 (C1)	30C	20%	1.4	5.2
3,2 (C2)	30C	66%	1.6	4
3,3 (C3)	37C	66%	3	6

REFERENCES

1. Baquero, F., Martinez, J.L. & Canton, R. Antibiotics and antibiotic resistance in water environments. *Current opinion in biotechnology* **19**, 260-265 (2008).
2. Gullberg, E. et al. Selection of Resistant Bacteria at Very Low Antibiotic Concentrations. *PLOS Pathogens* **7**, e1002158 (2011).
3. Molina-Quiroz, R.C. et al. Cyclic AMP Regulates Bacterial Persistence through Repression of the Oxidative Stress Response and SOS-Dependent DNA Repair in Uropathogenic Escherichia coli. *mBio* **9** (2018).
4. Cohen, N.R., Lobritz, M.A. & Collins, J.J. Microbial persistence and the road to drug resistance. *Cell host & microbe* **13**, 632-642 (2013).
5. Allison, K.R., Brynildsen, M.P. & Collins, J.J. Metabolite-enabled eradication of bacterial persisters by aminoglycosides. *Nature* **473**, 216 (2011).
6. Brauner, A., Fridman, O., Gefen, O. & Balaban, N.Q. Distinguishing between resistance, tolerance and persistence to antibiotic treatment. *Nature Reviews Microbiology* **14**, 320 (2016).
7. Bielicki, J.A. et al. Not too little, not too much: problems of selecting oral antibiotic dose for children. *BMJ : British Medical Journal* **351** (2015).
8. Bailey, A.M., Stephan, M., Weant, K.A. & Justice, S.B. Dosing of Appropriate Antibiotics and Time to Administration of First Doses in the Pediatric Emergency Department. *The journal of pediatric pharmacology and therapeutics : JPPT : the official journal of PPAG* **20**, 309-315 (2015).
9. Iizumi, T., Battaglia, T., Ruiz, V. & Perez Perez, G.I. Gut Microbiome and Antibiotics. *Archives of medical research* **48**, 727-734 (2017).
10. Rautio, J., Meanwell, N.A., Di, L. & Hageman, M.J. The expanding role of prodrugs in contemporary drug design and development. *Nature Reviews Drug Discovery* **17**, 559 (2018).
11. Al-Badr, A.A. & Ajarim, T.D.S. in Profiles of Drug Substances, Excipients and Related Methodology, Vol. 43. (ed. H.G. Brittain) 1-208 (Academic Press, 2018).
12. Baltzer, B. et al. Mutual pro-drugs of beta-lactam antibiotics and beta-lactamase inhibitors. *J Antibiot (Tokyo)* **33**, 1183-1192 (1980).
13. Zhang, L.-j. & Gallo, R.L. Antimicrobial peptides. *Current Biology* **26**, R14-R19 (2016).
14. Mahlapuu, M., Håkansson, J., Ringstad, L. & Björn, C. Antimicrobial Peptides: An Emerging Category of Therapeutic Agents. *Frontiers in Cellular and Infection Microbiology* **6** (2016).
15. Wimley, W.C. & Hristova, K. Antimicrobial Peptides: Successes, Challenges and Unanswered Questions. **239**, 27-34 (2011).
16. Bradshaw, J. Cationic antimicrobial peptides : issues for potential clinical use. *BioDrugs : clinical immunotherapeutics, biopharmaceuticals and gene therapy* **17**, 233-240 (2003).
17. Kwong, G.A. et al. Mass-encoded synthetic biomarkers for multiplexed urinary monitoring of disease. *Nat Biotech* **31**, 63-70 (2013).
18. Holt, B.A. et al. Fc microparticles can modulate the physical extent and magnitude of complement activity. *Biomaterials science* **5**, 463-474 (2017).
19. Holt, B.A., Mac, Q.D. & Kwong, G.A. Nanosensors to Detect Protease Activity In Vivo for Noninvasive Diagnostics. *JoVE*, e57937 (2018).
20. Mac, Q.D. et al. Non-invasive early detection of acute transplant rejection via nanosensors of granzyme B activity. *Nature biomedical engineering* (2019).
21. Lopez-Otin, C. & Bond, J.S. Proteases: multifunctional enzymes in life and disease. *The Journal of biological chemistry* **283**, 30433-30437 (2008).
22. Zhuang, Q., Holt, B.A., Kwong, G.A. & Qiu, P. Deconvolving multiplexed protease signatures with substrate reduction and activity clustering. *bioRxiv*, 564906 (2019).
23. Frees, D., Brondsted, L. & Ingmer, H. Bacterial proteases and virulence. *Sub-cellular biochemistry* **66**, 161-192 (2013).

24. Ingmer, H. & Brondsted, L. Proteases in bacterial pathogenesis. *Research in microbiology* **160**, 704-710 (2009).
25. Culp, E. & Wright, G.D. Bacterial proteases, untapped antimicrobial drug targets. *The Journal Of Antibiotics* **70**, 366 (2016).
26. Brannon, J.R. et al. Inhibition of outer membrane proteases of the omptin family by aprotinin. *Infection and immunity* **83**, 2300-2311 (2015).
27. McCarter, J.D. et al. Substrate Specificity of the Escherichia coli Outer Membrane Protease OmpT. *Journal of Bacteriology* **186**, 5919-5925 (2004).
28. Grodberg, J. & Dunn, J.J. ompT encodes the Escherichia coli outer membrane protease that cleaves T7 RNA polymerase during purification. *Journal of Bacteriology* **170**, 1245-1253 (1988).
29. Olson, E.S. et al. In vivo characterization of activatable cell penetrating peptides for targeting protease activity in cancer. *Integrative biology : quantitative biosciences from nano to macro* **1**, 382-393 (2009).
30. Franzman, M.R. et al. Targeted antimicrobial activity of a specific IgG-SMAP28 conjugate against Porphyromonas gingivalis in a mixed culture. *International journal of antimicrobial agents* **33**, 14-20 (2009).
31. Fujikawa, H., Kai, A. & Morozumi, S. A new logistic model for bacterial growth. *Shokuhin eiseigaku zasshi. Journal of the Food Hygienic Society of Japan* **44**, 155-160 (2003).
32. Ishihama, Y. et al. Protein abundance profiling of the Escherichia coli cytosol. *BMC Genomics* **9**, 102 (2008).
33. Roversi, D. et al. How Many Antimicrobial Peptide Molecules Kill a Bacterium? The Case of PMAP-23. *ACS Chemical Biology* **9**, 2003-2007 (2014).
34. Needham, D., Anyarambhatla, G., Kong, G. & Dewhirst, M.W. A new temperature-sensitive liposome for use with mild hyperthermia: characterization and testing in a human tumor xenograft model. *Cancer research* **60**, 1197-1201 (2000).
35. Kramer, R.A., Zandwijken, D., Egmond, M.R. & Dekker, N. In vitro folding, purification and characterization of Escherichia coli outer membrane protease ompT. *European journal of biochemistry* **267**, 885-893 (2000).
36. Kramer, R.A. et al. Identification of essential acidic residues of outer membrane protease OmpT supports a novel active site. *FEBS letters* **505**, 426-430 (2001).
37. Jin, D.J., Cagliero, C. & Zhou, Y.N. Growth rate regulation in Escherichia coli. *FEMS microbiology reviews* **36**, 269-287 (2012).